FULL SCALE TURBINE-MISSILE CASING EXIT TESTS

H. R. YOSHIMURA, J. T. SCHAMAUN
Sandia Laboratories, Albuquerque, New Mexico 87185, U.S.A.

G. E. SLITER
Electric Power Research Institute,
P.O. Box 10412, Palo Alto, California 94303, U.S.A.

Two full-scale tests have simulated the impact of a fragment from a failed turbine disk upon the steel casing of a low-pressure steam turbine with the objective of providing data for making more realistic assessments of turbine missile effects for nuclear power plant designers. Data were obtained on both the energy-absorbing mechanisms of the impact process and the post-impact trajectory of the fragment.

In both tests the target structure was a simplified model of a casing. The two main semicircular casing components that are expected to absorb most of the energy in a postulated failure were modeled: the internal blade ring which supports the stationary turbine blades (represented by a 12.7-cm-thick steel ring) and the outer casing cover (represented by a 3.2-cm-thick steel shell).

The missile in both tests was a 120° segment of a last-stage, shrunk-on turbine disk with a mass of 1526 kg. The segment had no blades since it is assumed that the blades would be broken off or crushed during exit. The rotation of the segment was not simulated in the tests. Instead, the total translational and rotational energy of the hypothetical turbine segment was included in the translational energy of the test missile.

In each test the missile was propelled by a rocket sled to impact the target structure at a nominal speed of 146 m/s. This translational velocity gives the same total kinetic energy (16.4×10^6 J) as a 120°-, 1526-kg segment leaving a shaft spinning at 120 percent of operational speed (the "design overspeed" condition). Since the orientation of a turbine segment at impact with the inner ring has a great influence on the absorbed energy, the missile had a "bounding" orientation for each test. In the first test, a "piercing" orientation with sharp corner impact and minimum projected area was selected to give a low estimate on absorbed energy. In the second test, a "blunt" orientation, 90° to the first, with curved-edge impact and maximum projected area, was selected to give a high estimate on absorbed energy.

In the test with piercing orientation, the missile perforated both structures and exited with a velocity of 87 m/s. In slowing the missile to 60 percent of its initial speed, the casing structures absorbed two-thirds of the missile's energy. After penetrating and exiting the simulated casing, the segment was rotating at 115 rpm.

In the test with blunt orientation, the missile did not perforate either the ring or the shell. Instead, the momentum transferred to the structures failed the bolts at their end supports and the net energy dissipated brought the missile almost to rest.

The tests demonstrated that turbine casings can absorb substantial amounts of energy in slowing down or containing fragments from a postulated turbine failure. Additional testing and analysis are needed to quantify the energy that can be dissipated over a full range of impact conditions and to examine the possible mitigating effects of fragment rotation and off-normal orientation on subsequent impacts on outer concrete walls of power plants.

*This work is supported by EPRI and is performed by Sandia under DOE contract.

1. Introduction

Nuclear power plant designers are required to provide adequate protection for safety-related components against the effects of postulated high-energy turbine missiles [1]. These missiles could be produced by the unlikely failure of shrunk-on disks that support the rotary blades of large steam turbines.

In plants with a "peninsula" arrangement, protection is provided by installing the turbine axis radially from the reactor building, so that potential missile trajectories are not in line with the plant. In plants with a "non-peninsula" arrangement (turbine axis perpendicular to a radius), designers rely on the low probability of a missile strike and on the protection afforded by reinforced concrete walls to demonstrate an adequate level of protection.

One of the critical first steps in demonstrating the adequacy of such protection is the determination of the energy of turbine segments as they exit the turbine casing. Two full-scale turbine casing exit tests have been completed at the rocket sled track facility of Sandia Laboratories, Albuquerque, New Mexico. The objective was to provide benchmark data on both the energy-absorbing mechanisms of the impact process and, if breakthrough occurred, the exit conditions of the fragment. This test series was sponsored by the Electric Power Research Institute (EPRI).

2. Test Description

The tests simulated the impact of a fragment from a failed shrunk-on turbine disk on the internal stator blade ring and on the outer wall of a low-pressure turbine casing. Because of wide variations in turbine designs, postulated failure conditions, and missile exit scenarios, the conditions for the two tests were carefully selected to give a first-order simulation of prototypical conditions while maintaining the well-characterized conditions needed for generating benchmark data.

3. Target Structure

The target structure in both tests simulated the upper halves of the internal rings and outer casings of the low-pressure section of a large 1800-rpm steam turbine (Figure 1). The inner structure, representing a last-stage stationary-blade support ring, was 12.7 cm thick, 50.8 cm wide, and 431.8 cm in diameter. The outer shell, representing a casing cover, was 3.2 cm thick, 182.9 cm wide, and 635 cm in diameter. The ring and the shell were fabricated from ASTM A515 Grade 65 cold-rolled steel with a tensile yield of 300 MPa, a tensile ultimate of 491 MPa, and an elongation of approximately 26% at room temperature. Standard Charpy-V specimens from the ring material gave an energy of 20 J at 38°C. These two turbine components represent the main energy-absorbing and trajectory-deflecting members in a postulated failure.

The ring and the shell were bolted to a massive concrete structure and soil overburden weighing 1633 metric tons. The bolted connections simulated as closely as practicable the horizontal joints in an actual turbine. Twelve 3.8-cm-diameter bolts held down each end of the ring; these had an ultimate strength of 11.5 MN and an active length of 25.4 cm. Fourteen 2.54-cm-diameter bolts held down each end of the shell; these had an ultimate strength of 6.7 MN and an active length of 15.2 cm. All bolts were fabricated from A490

steel. The ring was maintained near 38°C, typical of the temperature in the last stage region of an operating turbine.

4. Missile Impact Conditions

The test missile was selected from amongst the heavier-weight missiles considered in design. The missile in both tests was a 120° sector of a last-stage shrunk-on disk manufactured by Westinghouse Corporation. (This missile was selected from among several turbine disk segments provided for the test program by Westinghouse and General Electric Company.) Dimensions and mass properties of the 1527-kg missile are given in Figure 2. The missile was made from high-strength alloy steel (ultimate strength of 896 MPa). Note that the turbine sector has no blades; it is assumed that the blades break off or are crushed during exit.

The missile was mounted on a lightweight support sled, which was pushed by a rocket sled (Figure 3). After the acceleration stage the rocket sled was braked, allowing the missile and support sled to coast toward the target. Activation of explosive bolts just before impact separated the missile from the support sled, which was diverted by a striker plate beneath the target structure. The missile then traveled in free flight before its 15.5-cm-wide edge struck the center of the 50.8-cm-wide ring. As indicated in Figure 1, the flight path of the missile's center of gravity was offset 51.3 cm from the centerline of the track and the structure. This simulated the trajectory of a turbine segment that leaves the shaft translating tangentially from a circle through the segment's center of gravity. The rotation of the segment, which would be initially at the rotational velocity of the turbine at failure, was not simulated in the tests. Instead, the total translational and rotational energy of the hypothetical turbine segment was included in the translational energy of the test missile.

The nominal impact velocity in both tests was 146 m/s. This translational velocity gave the same total kinetic energy (16.4×10^6 J) as a segment leaving a shaft spinning at 2160 rpm, or 120% of operating speed (the "design overspeed" condition).

Since the orientation of a turbine segment at impact with the inner casing ring cannot be specified with certainty and since orientation has a large influence on absorbed energy, the missiles in the two tests had "bounding" orientations (Figure 1). In the first test a piercing orientation, with sharp corner impact and minimum projected area, gave a low estimate on absorbed energy. In the second test a blunt orientation, 90° to the first, with curved edge impact and maximum projected area, gave a high estimate on absorbed energy.

5. Test Results

In the test with a piercing orientation, the missile penetrated about 10 cm into the ring, broke through both the ring and the shell, and exited with a translational velocity of 86.9 m/s (Figure 4a, b, c). After failure of the ring at the impact point, both ends of the ring broke at the edge of the welded gusset plates that connected the ring to its base plate. The bolts connecting the base plate to the backup structure did not fail.

A plot of missile displacement versus time taken from an overhead high-speed camera is shown in Figure 5, and missile velocity and energy at various times are summarized in Table I. Further evaluation of the data in Table I shows that (1) in slowing the missile to

58% of its initial speed, the structure absorbed two-thirds of the missile's energy; and (2) 85% of the absorbed energy was dissipated by ring impact and only 15% by shell impact.

The segment was rotating at 115 rpm after exiting the simulated casing (Figure 4c). The rotational energy imparted to the missile was negligible (0.6%) compared with the total exit energy. The missile was only slightly deformed by the impact; the sharp corner was blunted about 2.5 cm.

Samples of the records from 26 strain gages on the ring and the shell are given in Figures 6 and 7. The gage in Figure 6 measured circumferential membrane strain on the mid-surface of the ring at a cross section through the impact point. A tensile strain of about 1.3% was measured before the gage failed at less than 1 ms (ring fracture occurred between 2.1 and 2.5 ms after impact). The maximum strain rate measured was 64 s^{-1}.

The gage in Figure 7 measured circumferential membrane strain at a cross section 12.1° from the support closest to the impact point. The strain peaked at about 2 ms after impact and began oscillating around a small residual strain at about 3 ms, when high-speed photography showed fracture at the nearby support. The peak reaction load, estimated from strain measurements, was approximately 14.6 MN.

In the test with a blunt orientation, the missile did not perforate either the ring or the shell (Figure 8a, b, c). Instead the momentum transferred to the structures failed all of the support bolts, and the net energy dissipated brought the missile almost to rest. As indicated by the displacement, velocity, and energy histories in Figure 9 and Table II, 95% of the missile's initial energy was dissipated as the ring impact slowed the missile to one-fifth of its initial speed. Missile velocity remained constant until impact with the shell which absorbed virtually all of the remaining 5% of its energy.

Sample strain records are given in Figures 10 and 11. The gage in Figure 10 measured circumferential strain in the ring near the impact point (52° from the support). A peak strain of about 0.8% was measured before the gage failed at 6 ms.

The gage in Figure 11 measured circumferential strain at a cross section 12.1° from the support closest to the impact point. The strain peaked at 7 ms after impact, which is the approximate time that high-speed photography showed bolt failure at the nearby support. The peak reaction load, estimated from strain measurements, was approximately 19.0 MN.

In a final report [2], detailed data from both tests are presented and compared with preliminary calculations. This report includes estimates of the amount of energy dissipated by various momentum transfer and energy absorption processes. The data will provide a benchmark for various calculational techniques used in design. Plans are being considered for additional testing and analysis.

Results of the tests described above will also provide a basis for selecting missile velocities to be used for concrete structure impact tests scheduled to begin in late 1979.

References

[1] Nuclear Regulatory Commission, "Protection Against Low-Trajectory Turbine Missiles," Regulatory Guide 1.115, Revision 1, July 1977.

[2] Yoshimura, H. R., and Schamaun, J. T., "Full Scale Turbine Missile Casing Tests," EPRI Final Report (1979) in press.

Table I

MISSILE ENERGY, PIERCING ORIENTATION

Event	Time (ms)	Measured Velocity (m/s)	Kinetic Energy (MJ)	Cumulative Energy Dissipation (%)
Ring impact	0	149	17.0	0
Ring fracture to shell impact	2.5-9.5	99	7.5	56
After shell perforation	20	87	5.7	66

Table II

MISSILE ENERGY, BLUNT ORIENTATION

Event	Time (ms)	Measured Velocity (m/s)	Kinetic Energy (MJ)	Cumulative Energy Dissipation (%)
Ring impact	0	151	17.4	0
Ring bolt failure to shell impact	9-18	32	0.8	95
Shell bolt failure	55	8	0.04	99.7

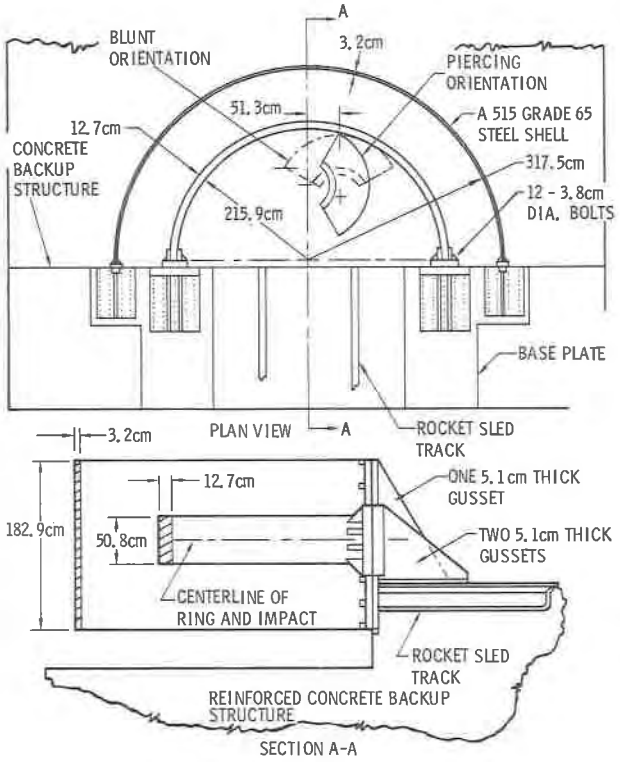

Figure 1 Target structure, missile, and impact orientations

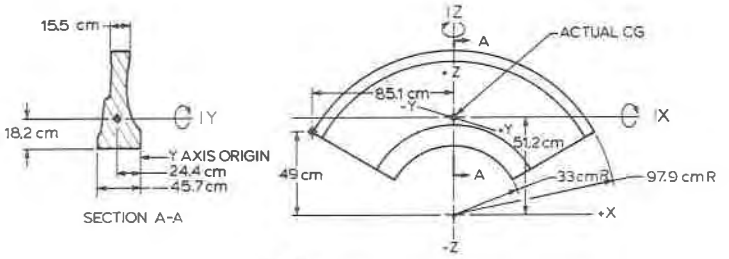

Weight: 1,526.7 Kg
Center of gravity: X=0, Y=24.4cm; Z=51.2cm
Mass moment of inertia: IX = 63.4 Kg-m²
IY = 239.5 Kg-m²
IZ = 200.8 Kg-m²

Figure 2 Dimensions and mass properties of steel missile segment (120° hub section)

Figure 3 Missile, support sled, and rocket pusher sled

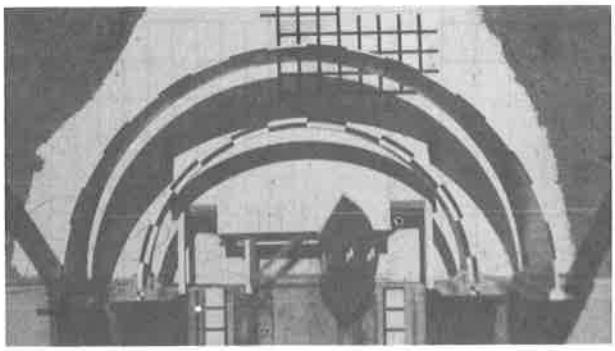

Figure 4a (V = 149 m/s, ω = 0)

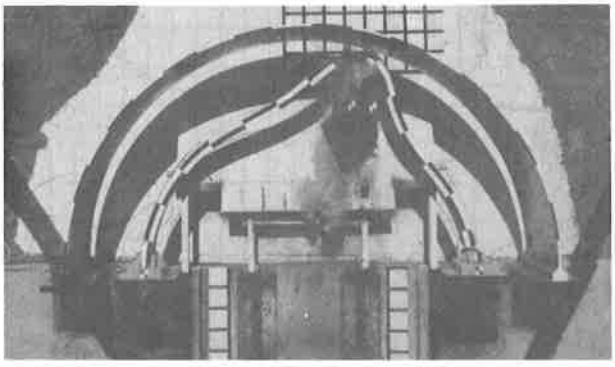

Figure 4b (V = 99 m/s)

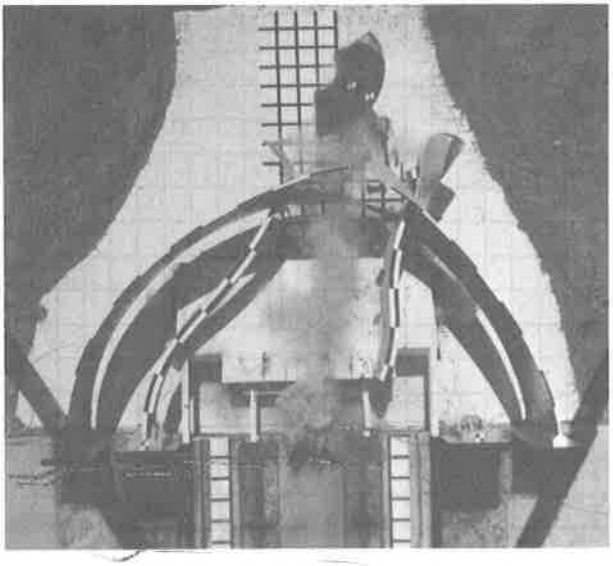

Figure 4c (V = 87 m/s, ω = 115 rpm)

Figure 4 Overhead photograph of piercing impact

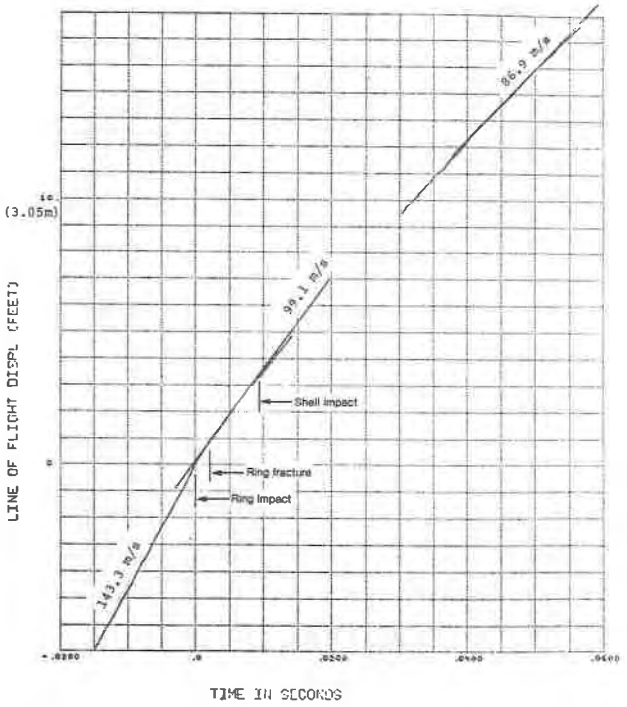

Figure 5 Displacement history of missile in test with piercing orientation(1 ft = 0.305 m)

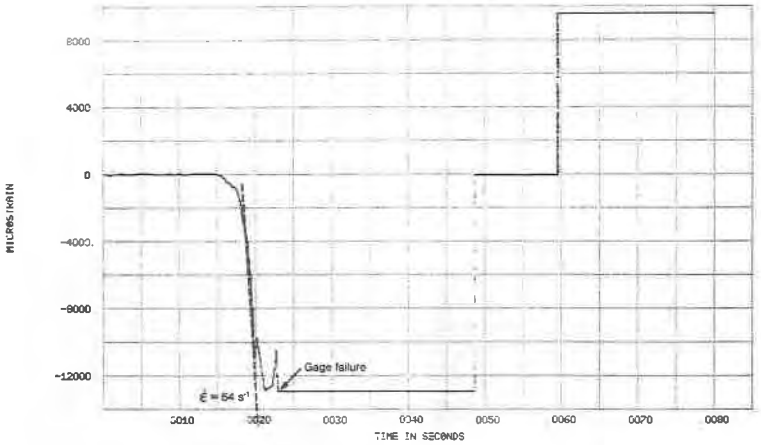

Figure 6 Strain record near impact point, piercing orientation (negative sign denotes tensile strain)

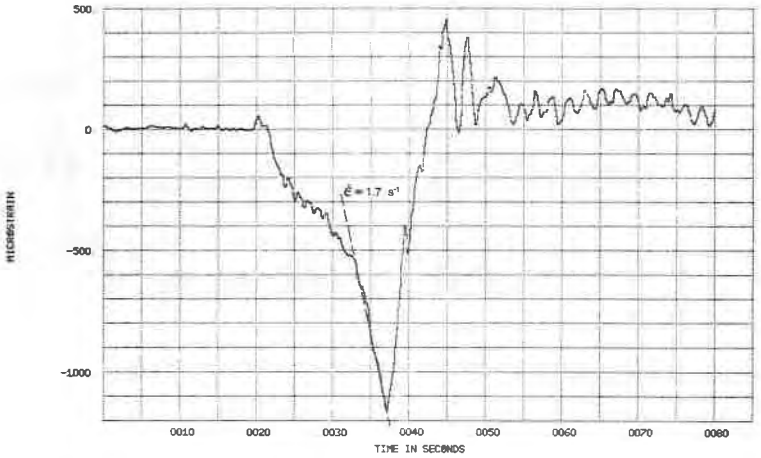

Figure 7 Strain record near support, piercing orientation (negative sign denotes tensile strain)

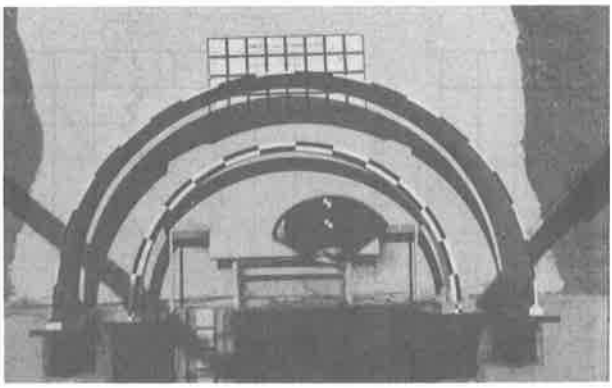

Figure 8a (V = 151 m/s, ω = 0)

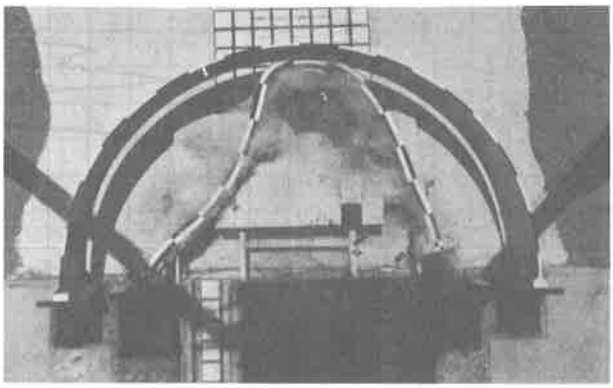

Figure 8b (V = 32 m/s)

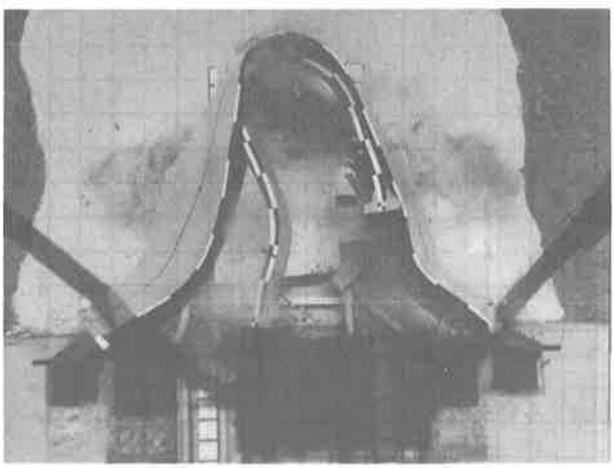

Figure 8c (V = 3 m/s, ω = 0)

Figure 8 Overhead photograph of blunt impact

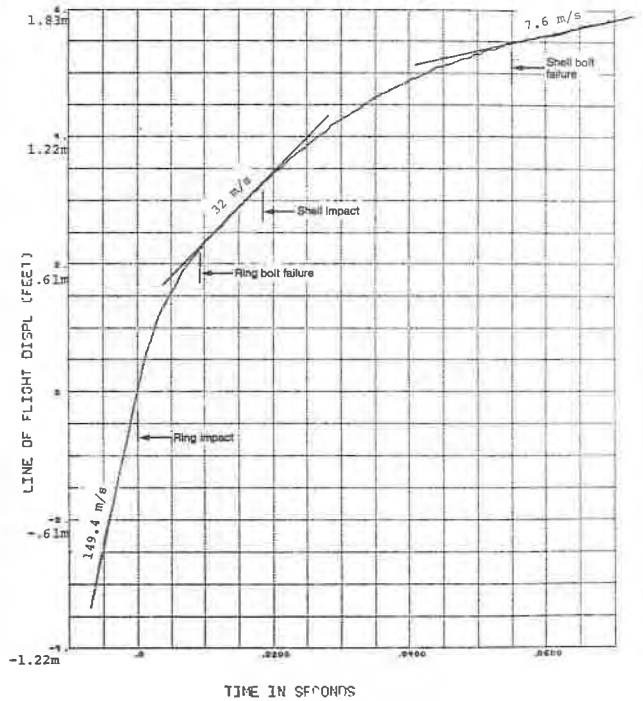

Figure 9 Displacement history of missile in test with blunt orientation (1 ft = 0.305 m)

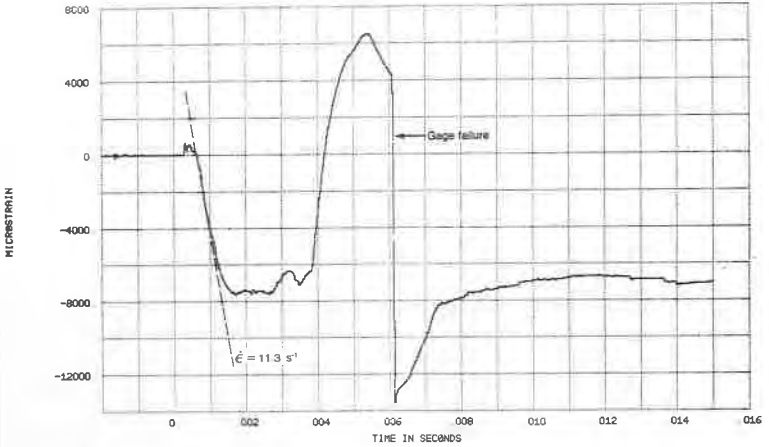

Figure 10 Strain record near impact point, blunt orientation (negative sign denotes tensile strain)

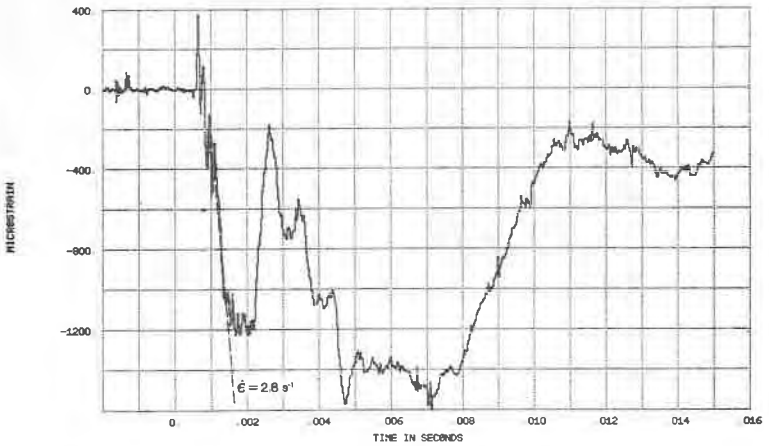

Figure 11 Strain record near support, blunt orientation (negative sign denotes tensile strain)